Heliyon 10 (2024) e39123

Contents lists available at ScienceDirect

Heliyon

journal homepage: www.cell.com/heliyon

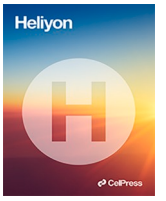

Research article

The adsorption mechanism and optimal dosage of walnut shell biochar for chloramphenicol

Caixia Sun [a,*], Gangjun Wang [a], Yuhong Liu [a], Ke Bei [b], Guoguang Yu [a], Weiran Zheng [a], Yuxue Liu [a]

[a] Institute of Agro-product Safety & Nutrition, Zhejiang Academy of Agricultural Sciences, Hangzhou, 310021, China
[b] College of Life and Environmental Science, Wenzhou University, Wenzhou, 325035, China

ARTICLE INFO

Keywords:
Walnut shell biochar (WSB)
Chlorantraniliprole (CAP)
Adsorption mechanism
Optimal use dosage

ABSTRACT

Biochar derived from biomass pyrolysis has proven to be an excellent material for pesticide adsorption and can be used as soil amendment for pesticide non-point pollution. However, the adsorption and desorption mechanisms for certain biochar and pesticide are still unclear. In this study, we investigated the properties of biochar derived from walnut (Juglans regia L.) shell (WSB), and used batch equilibrium method to investigate the adsorption and desorption behavior for chlorantraniliprole (CAP). The physical-chemical analysis showed that there were mainly lignin charcoal of alkyl carbon, methoxyl carbon, aromatic carbon, and carboayl carbon as the primary carbon compounds of WSB. The π - π electron donor acceptor interaction, electrostatic interaction, and hydrogen bond were the primary adsorption mechanisms of the WSB adsorption. Batch equilibrium study under 298 K showed that WSB application in the soil significantly improved the adsorption ability for CAP, and the adsorption behavior was a mono-layer adsorption process as Langmuir model fitted the adsorption isotherm data better than the Freundlich model. While Freundlich model analysis showed that WSB addition to the soil changed the isothermal adsorption line from the S style to the L style. The spontaneous degree reaction of sorbents from strong to weak was in the following order: 5%-WSB >7%-WSB >10%-WSB >1%-WSB >3%-WSB > soil > WSB, and the maximum application effect was achieved at 5 % (m/m) WSB dosage mixed with the soil. Therefore, we considered that WSB addition in soil increased its CAP adsorption capacity, and 5 % (m/m) WSB application was the best choice for CAP pollution control. These data will contribute to the adsorption mechanism and the optimal use dosage of WSB for CAP pollution control.

1. Introduction

Chlorantraniliprole (CAP) belongs to the group of diamide insecticides. It was developed by DuPont in 2007, and it is a widely used pesticide worldwide including in China [1–3]. CAP has been mainly registered in rice, corn, cotton, sugarcane, sorghum, and many other crops [4]. According to the statistics, worldwide sales of CAP was more than 2 billion dollars in 2023, and it has maintained the top sales position in the insecticide market for years [5]. However, excessive CAP application may cause environmental and health

* Corresponding author. Institute of Agro-product Safety & Nutrition Zhejiang Academy of Agricultural Sciences 198# Shiqiao Road, Hangzhou, Zhejiang, China.
E-mail address: suncaixia0571@126.com (C. Sun).

https://doi.org/10.1016/j.heliyon.2024.e39123
Received 11 May 2024; Received in revised form 7 October 2024; Accepted 8 October 2024
Available online 10 October 2024

impacts [6]. Researchers have found that CAP can adversely affect non-target organisms and harm the bacterial community in soil [7–9].

In modern agriculture, soil has an important position in the food-chain and planetary health system [10,11]. Maintaining soil health is important for sustaining agricultural development and food security [12,13]. Overused pesticides can enter not only the air and water but also the soil and persist for extended periods and cause non-point source (NPS) pollution such as soil health hazards, water quality declines, and crop quality reductions [14–16]. Here, NPS pollution refers to pollution from a broad group of human activities that does not have a single point of entry into environment [17]. Former studies have shown that CAP has a long half-life in the aqueous phase for 26 days, and in the benthic zones of flooded and drained fields, CAP has a half-life of 29 and 92 days, respectively [18]. CAP also showed cross resistant with other insecticides and poor ovipositor development in female insects for its long half-life characteristic [19]. CAP in soils also alters the bacterial and fungal community structures at low concentration levels from 0.8 mg/kg to 20 mg/kg [20]. Techniques for pesticide removal from soil are mainly physico-chemical approaches, such as photocatalytic degradation and advanced oxidation, and adsorption techniques [21–23]. The adsorption techniques to prevent or reduce pesticide migration from soils to plants should be easy to perform and are suitable for agricultural soil remediation.

Biochar is a multifunctional carbon-rich material, and it is derived from life activities and plant-derived agroforestry biomass wastes. Many agricultural production wastes, such as walnut (Juglans regia L.) shell, rice straw, wheat straw, corn straw, bamboo, and rice husk, can be used for biochar production [24,25]. The use of biochar in agriculture is of great significance for carbon sequestration, NPS pollution control, heavy metal pollution remediation, farmland and saline-alkali soil improvement, food security protection, and agricultural ecological environmental security protection [26–28]. As biochar possesses good adsorption ability, it has an obvious effect on pesticide environmental behavior control, including migration control in soil, the problem of reduced agriculture safety, and environmental safety problems caused by pesticides [29–31]. Studies have shown that biochar treatment is an effective method for pesticide adsorption in soil environments, and biochar addition to wetlands has been shown to be a promising approach for CAP mitigation for agricultural runoff waters [32,33].

Biochar addition in soil will change the soil characteristics, including its chemical adsorption ability [34,35]. Former studies of biochar in-situ remediation have shown that biochar addition in soil can alter pesticide environmental fate due to its adsorption ability and filtration in soil environments [36]. Adsorption isotherms and adsorption thermodynamic investigations are very important because these properties and data are the basis for the selection of a suitable sorbents, the design of the application dosage, and the economic analysis [37]. Pesticide adsorption in soil is a complex process and is affected by several factors, including the pesticide chemical properties, soil characteristics, and climatic factors [38].

The adsorption ability is affected by several factors, and the biochar application dosage is the most important [39]. Although the environmental behavior of pesticides under various conditions and soil factors have been studied, the interaction of the biochar-soil system and dosage optimization for biochar addition have not been well documented. In this study, we used the batch equilibrium method to study the walnut shell biochar (WSB) adsorption effect mechanism. WSB from walnut shell could be used as a raw material for the in-situ remediation of farmland pesticide pollution, as walnut is an important cash crop in Zhejiang Province and has the production of more than 0.5 million ton of each year and it is much more suitable for using as an alternate low-cost adsorbent material [40–42]. The batch equilibrium method is widely used to investigate chemical substances, including the pesticide migration rate and their distribution information in the soil, aquatic areas, and the biosphere [43]. The Organization for Economic Co-operation and Development (OECD) has published guide No. 106 for chemical adsorption desorption using the batch equilibrium method, and this method is identical to the Chinese national standard (GB/T 21851-2008) [44].

Former studies have shown that biochar made from the pyrolysis of agricultural wastes can be used as a high-efficiency sorbent for pesticide non-point pollution control [45–47]. However, the adsorption and desorption mechanisms for certain biochar and pesticide are still unclear, and the maximum application dosage is unknown in actual production. Based on the favorable characteristics of biochar on pesticide adsorption, the present studies have primarily focused on the effect of the biochar addition proportion to soil on the pesticide adsorption ability in soil. In general, the adsorption effect for pesticides in soil increases with biochar addition dosage and increases with the adsorption contact time [48]; and the effect of biochar application on the migration, transformation, and distribution of pesticides in soil and aquatic environments [49].

Therefore, in this study, we investigated the properties of WSB, and used batch equilibrium method to investigate the adsorption and desorption behavior of CAP on WSB. The experiment was carried out according to the OECD guideline 106 to elucidate the adsorption mechanism of CAP on WSB. From a management perspective, WSB from walnut shell was used as a raw material for the in-situ remediation of farmland, which had great importance for walnuts resource recycling. For the meaning of the study is concerned, from an applicability perspective, intensive efforts were necessary to investigate and maximize the performance of WSB application including optimal dosage. As such, this study has two objectives: (i) to investigate adsorption behavior for CAP in the sorbens with biochar and soil by using a kinetics model and a thermodynamic parameters analysis of the adsorption model; (ii) to investigate and maximize biochar addition dosage for CAP adsorption capacity in soil.

2. Experimental materials and methods

2.1. Experimental material

The WSB was supplied by the Zhejiang Biochar Engineering Center, Hangzhou city, Zhejiang province, and it was crushed and passed through an 80-mesh (with 0.32 mm diameter) sieve for later use. The WSB was produced at the highest treatment temperature of 450 °C for 3 h and at a heating rate of 5°C-10 °C/min. The physical and chemical properties of the WSB were as follows: Specific

surface area 89.85 m^2/g, pH value of 6.78, density of 0.33 g/ml, total nitrogen content of 1.26 %, available phosphorus content of 0.038 %, K content of 3.82 %, and total organic content (TOC) of 93.90 %.

The upper 15-cm layer of the soil was collected from the trial base of Zhejiang Academy of Agricultural Sciences, Hangzhou, China. When sampling the soil, the surface stones, leaves, and other impurities were removed, and a shovel was used to evenly sample the soil. The soil sample was air-dried and passed through an 80-mesh sieve (with 0.32 mm diameter) after being crushed. The physical and chemical properties of the soil were as follows: pH value of 6.52 (pH value was determined in 1.2 (soil: water) ratio using digital electronic pH meter), moisture content of 1.31 %, total organic content (TOC) of 2.91 % (TOC was determined by a volumetric technique), total nitrogen (TN) of 0.45 % (TN was determined using a San++ flow analyzer), available phosphorus (TP)_content of 0.011 % (TP was determined by phosphoric acid molybdenum antimony colorimetric method) [53], and available potassium (TK) content of 0.0081 % (TK was determined by standard soil testing procedures) [50–54].

The CAP standard of 97.84 % purity was supplied by Dr. Ehrenstorfer Co., Ltd, Germany. The acetonitrile, methanol, and toluene of chromatographic grade were supplied by Aladdin Reagent Co., Ltd, Shanghai, China. Water of chromatographic grade was supplied by Wahaha Co., Ltd, Hangzhou, China. $CaCl_2$ and NaN_3 of analytical grade were supplied by Aladdin Reagent Co., Ltd.

2.2. Walnut shell biochar characterization

Nuclear magnetic resonance (NMR) spectroscopy and X-ray diffraction (XRD) were used to characterize the WSB. NMR was detected using the Bruker AVANCE III 600 with an ultraviolet–visible (UV–VIS) spectrophotometric detector, and the resonance frequency was 150.9 MHz. The C CP/MAS NMR spectra were recorded using a 4-mm magic angle spinning (MAS) probe and a spinning rate of 14 kHz. A contact time of 2 ms and a recycle delay of 3 s were used for the ^1H-^{13}C CP/MAS measurement.

2.3. Batch equilibrium method

The distribution of a chemical between soil and aqueous phases is a complex process depending on a number of different factors: the chemical nature of the substance, the characteristics of the soil, and so on. We conducted the batch equilibrium experiments according to the OECD guideline 106. According to this guideline, adsorption represents the process of the binding of a chemical to surfaces of soils. The test is designed to evaluate the adsorption of a chemical on different soil types with a varying range of organic carbon content.

In preliminary experiment, 1 kg air-dried soil was prepared and 1 %, 3 %, 5 %, 7 %, and 10 % weight proportion WSB were mixed with the soil fully, and 60 % saturated moisture was added. The samples were left for 21 days in an incubator at 25 °C prior to aging. Sorbents, including soil only, biochar only, and the biochar-soil mixtures with 1%-WSB, 3%-WSB, 5%-WSB, 7%-WSB, 10%-WSB dosage were mixed together with the CAP solution. A stock solution of CAP at a concentration of 1000 mg/L was prepared in methanol and stored at 4 °C in the dark. The CAP was diluted in a solution containing 0.01 M $CaCl_2$ and 0.20 g/L NaN_3 to maintain a constant ionic strength and to inhibit microbial activities.

Sorbents (mixture of different proportion WSB with soil) of 1.00 g were weighed, and 50 mL CAP solutions with initial concentrations of 5, 10, 15, 20, and 25 mg/L were added to the sorbents in 50-mL centrifuge tubes with five replicates. All the tubes were shaken at 25 °C for 24 h at 120 rpm. The tubes were then centrifugated for 10 min at 3000 rpm. Approximately 1–2 mL of supernatant was withdrawn from each sample using an injector, filtered through a 0.45-μm membrane, and added to 1.5-mL vials to analyze the CAP concentration in the solution phase using high performance liquid chromatography (HPLC). The remaining soil phase was kept for the subsequent desorption experiments.

The desorption experiments were conducted immediately after adsorption procedure. As much of the remaining supernatant was removed from the tubes as possible; then, 50 mL of a fresh background solution (0.01 M $CaCl_2$ without CAP) was added to the centrifuge tubes. The tubes were shaken at 25 °C for 24 h and centrifuged; then, the supernatant was collected to analyze the CAP concentration in the aqueous phase using HPLC. The desorbed CAP amount was calculated from the CAP concentration in the aqueous phase.

In the preliminary tests, the adsorption equilibrium analyses of CAP in the soil alone, in biochar-soil mixtures, and in the biochar alone were performed at an initial concentration of 10 mg/kg. Equilibrium was achieved for all experiments within 24 h.

The adsorption quantity was calculated using the following equation:

$$q_e = \frac{(C_0 - C_e)V}{m}, \tag{1}$$

where q_e is the CAP quantity of WSB adsorbed on the soil/WSB (mg/kg); C_0 is the initial concentration of CAP; and C_e is the CAP concentration at sampling equilibrium moment.

The desorption quantity was calculated using the following equation:

$$C_{dq} = \frac{C_{de}V}{m}, \tag{2}$$

where C_{dq} is the CAP quantity of WSB desorbed from the soil/WSB (mg/kg); and C_{de} is the CAP concentration at equilibrium moment.

Freundlich and Langmuir isotherm non-linear models are used to determine the relationship between the adsorbate in the aqueous solvent phase and the adsorbate adsorbed on the surface of the adsorbent at equilibrium and constant temperature.

Freundlich model is expressed as the follows:

$$\lg q_e = \lg K_f + 1/n \lg C_e, \tag{3}$$

where q_e is the amount of CAP absorbed on the WSB (mg/kg), and is equal to q_e in equation (2); C_e is the equilibrium solution adsorbed concentration (mg/L), and is equal to C_e in equation (2); and K_f and 1/n represent the rate constant of adsorption [55].

Langmuir model is expressed as follows:

$$\frac{1}{q_e} = \frac{1}{Q_{max}} + \frac{1}{K_L Q_{max} C_e}, \tag{4}$$

where q_e is the amount of CAP absorbed on the WSB (mg/kg), and is equal to q_e in equation (2); C_e is the equilibrium solution adsorbed concentration (mg/L); Q_{max} is the maximal mono-layer adsorption amount; and the parameter K_L represents the rate constant of adsorption [56].

The influence of WSB addition in soil at 298 K was calculated using the equations below:

$$\Delta G^{\ominus} = -RT\ln K_{oc} \tag{5}$$

$$K_{oc} = K_f / f_{oc}, \tag{6}$$

Where $\Delta G^{\ominus}$ is the Gibbs free energy change; R is a constant (8.314 J/mol·K); f_{oc} is the organic content of the biochar-soil mixture; K_f is the constant value in Freundlich model; and K_{oc} is the constant corrected for organic matter content.

2.4. CAP analysis using HPLC

Thermo HPLC with an Agilent C_{18} column (250 mm × 4.6 mm) and an ultraviolet (UV) detector was performed for analyzing the CAP concentration in the batch adsorption studies. The mobile phase consisted of 80 % acetonitrile and 20 % water at a flow rate of 0.5 mL/min. The detection wavelength for the UV detector was set at 265 nm. The injection volume was 10 μL. The detection limit of CAP was 0.05 mg/L. A good linear correlation was obtained for CAP. The equation was $Y = 0.92X + 0.0032$, with a correlation coefficient (R^2) of 0.999 at five concentrations (0.01, 0.1, 1.0, 5.0, and 10 mg/kg) with three replicates.

2.5. Statistical analysis

Statistical analysis was performed using Microsoft Excel 2015 (Microsoft Corporation, USA) and SPSS 19.0 (International Business Machines Corporation, USA).

3. Results and discussion

3.1. NMR and XRD characterization results

The NMR and XRD characterization results of WSB are shown in Figs. 1 and 2.

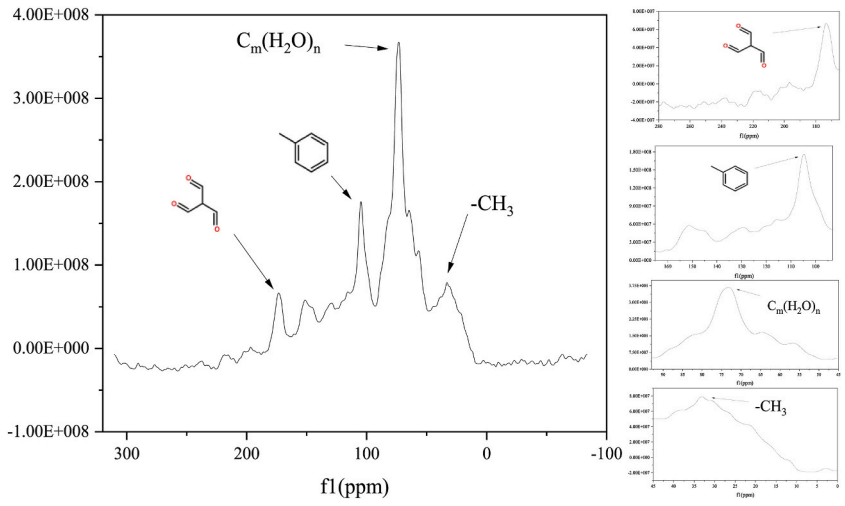

Fig. 1. Nuclear magnetic resonance (NMR) curve of the WSB characterization.

Fig. 1 shows that there were four main regions of the spectrum information regarding the overall structure of the WSB. The chemical shifts between 0 and 45 ppm were likely related to alkyl carbon, and those between 45 and 93 ppm were likely related to methoxyl carbon and carbohydrate. Aromatic carbon was present between 93 and 165 ppm, and carboayl carbon was present between 165 and 280 ppm.

The XRD spectra were recorded on an X-ray powder diffractometer using CuKα radiation operating at 40 kV and 30 mA. The powder samples were placed on an aluminum slide with a 2-mm-thick layer. The samples were scanned at a reflection angle of 2θ using a step rate of 0.5°/min.

Fig. 2 shows the XRD curve of the WSB. We analyzed the results using Jade 6.0 software, which showed that the hkl values were 113, 300, 401, 511, and 452 for the 2θ values of 21, 27.5, 40, 50, and 68, respectively. The weak diffraction was expected for the non-graphitizable carbonized cellulosics, and the broader peaks at 21° and 27.5° that obtained were consistent with the presence of amorphous carbon and/or the presence of nanoparticles. The XRD analysis results showed that the WSB consisted of large amounts of lignin charcoal other than crystalline carbon.

WSB characterization showed that there was a large amount of lignin that remained in the material. During WSB production, alkyl carbon, methoxyl carbon, aromatic carbon, and carboayl carbon remained in the biochar material. Compared with crystalline carbon, the lignin charcoal had more alkyl carbon, methoxyl carbon, aromatic carbon, and carboayl carbon. The π - π electron donor acceptor interaction, electrostatic interaction, and hydrogen bond were the primary adsorption sites of the WSB adsorption [57].

3.2. Batch equilibrium method and adsorption thermodynamic

The batch adsorption-desorption results for CAP in the soil only, mixtures of soil and WSB, and WSB only are shown in Figs. 3 and 4, and the Supplementary Information S1 and S2. Fig. 3 shows that in adsorption procedure, CAP reaches adsorption equilibrium in short time (10 min), and therefore, it can be ruled out that the concentration reduction of CAP in the aqueous phase is caused by the adsorption of CAP in soil and biochar itself, rather than degradation itself. WSB addition in soil improves the adsorption ability of soil to CAP.

Fig. 4 shows the desorption procedure of CAP in soil and the mixture of soil and WSB. The rate of desorption fitted first-order well. As Fig. 4 and Table 1 show, if we compare the desorption data of course, the K_f value for the WSB, 1%-WSB, 3%-WSB, 5%-WSB, 7%-WSB, 10%-WSB and soil, were 4.98, 50.20, 50.22, 73.12, 49.20, 63.42 and 49.82, respectively. The desorption procedure of the 5%-WSB and 7-WSB showed easier to carry out desorption procedure. The result shows that there is hysteresis phenomenonin desorption procedure, which means different results between the measurements of the adsorption and desorption processes are obtained [58,59]. As the reasons are concerned, WSB has large specific surface area (89.85 m^2/g), and the adsorption procedure often occurs in the WSB micropores, and the π-π electron donor acceptor interaction causes the micropores filled with CAP absorbed on the adsorption sites, and it is hard to release during desorption process [60,61].

Using equations (1), (2) and (5), (6), the thermodynamic parameters for the adsorption of CAP in the soil/WSB are shown in Table 1.

The ΔG value is generally regarded as an indicator of the energy change during the adsorption-desorption process [62]. Table 1 showed that the ΔG value varied from −10.08 kJ/mol to −15.41 kJ/mol. When the absolute value of $\Delta G^{\ominus}$ was larger, the reaction driving force is stronger, and the adsorption reaction proceeded more easily [63]. Absolute values of ΔG less than 20 kJ/mol indicated that the equilibrium process may have involved physisorption as well as chemisorption. The K_f value of the soil was 1.32, while the value for the WSB was 485.20. The addition of WSB to the soil significantly increased the sorption capacity of the WSB. For the 1%-WSB, 3%-WSB, 5%-WSB, 7%-WSB, and 10%-WSB, the K_f values were 16.32, 20.71, 35.11, 39.32, and 48.72, which were 12.36,

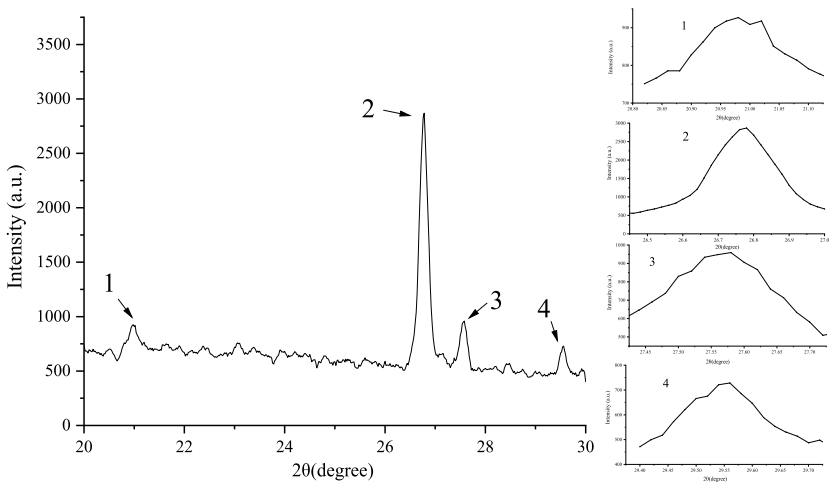

Fig. 2. X-ray diffraction (XRD) curve of the WSB characterization.

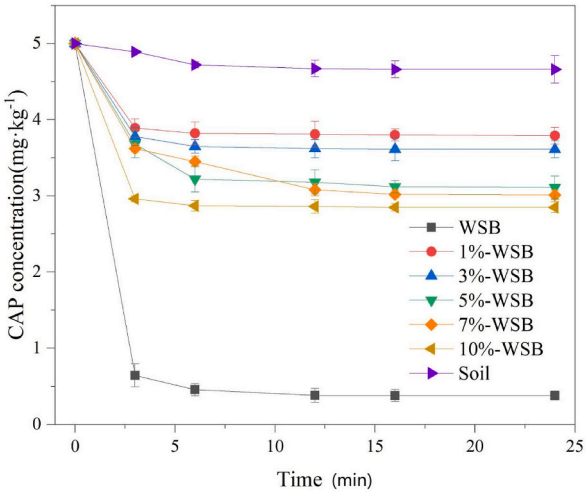

Fig. 3. Adsorption equilibrium of CAP with time.

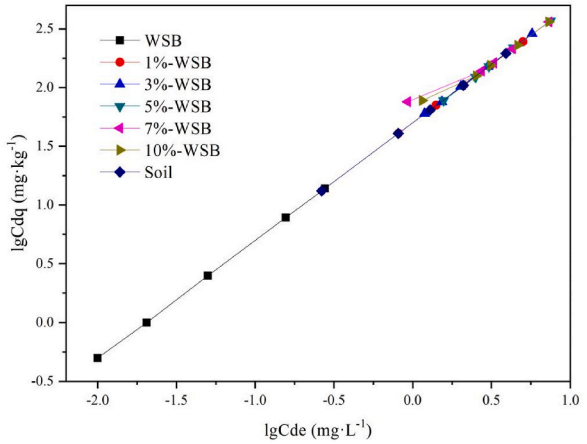

Fig. 4. Desorption of CAP in the soil only, mixture of soil and WSB, and the WSB only.

Table 1
Thermodynamic parameters for the adsorption of chlorantraniliprole (CAP) in the soil/walnut-shell biochar (WSB).

Procedure and material		Equation	K_f	f_{oc}	1/n	K_{oc}	ΔG°/(KJ mol^{-1})
Adsorption	WSB	Y = 0.64x+2.68	485.20	0.940	0.64	501.24	−15.41
	1%-WSB	Y = 0.92x+1.21	16.32	0.027	0.92	18.15	−7.18
	3%-WSB	Y = 0.86x+1.32	20.71	0.036	0.86	23.74	−7.85
	5%-WSB	Y = 0.77x+1.54	35.12	0.045	0.77	40.86	−9.19
	7%-WSB	Y = 0.76x+1.59	39.32	0.054	0.76	44.36	−9.39
	10%-WSB	Y = 0.74x+1.68	48.72	0.068	0.74	50.99	−9.74
	Soil	Y = 1.65x+0.12	1.32	0.023	1.65	58.41	−10.08
Desorption	WSB	Y = 1.01x+0.69	4.98	0.940	1.01	5.30	−4.13
	1%-WSB	Y = 0.98x+1.70	50.20	0.027	0.98	1873.11	−18.71
	3%-WSB	Y = 1.01x+1.70	50.22	0.036	1.01	1406.22	−17.90
	5%-WSB	Y = 0.74x+1.86	73.12	0.054	0.74	1351.22	−17.81
	7%-WSB	Y = 1.01x+1.69	49.20	0.045	1.01	1098.22	−17.30
	10%-WSB	Y = 0.84x+1.81	63.42	0.068	0.84	926.90	−16.90
	Soil	Y = 0.99x+1.69	49.82	0.023	0.99	2203.50	−19.10

15.68, 26.59, 29.78, and 36.90 times larger than K_f value of soil. In contrast, the desorption isotherms fitted the Freundlich model well, and the K_f values for the soil only and soil and WSB mixtures were greater than that of the soil only. For WSB, 1%-WSB, 3%-WSB, 5%-WSB, 7%-WSB, 10%-WSB, and soil, the K_f values were 4.98, 50.20, 50.22, 73.12, 49.20, 63.42, and 49.82, respectively. The results

indicated that CAP sorption in the soil was largely irreversible, while for the mixture of soil and WSB, sorption was reversible. During the desorption procedure, the ΔG values varied from −4.13 to −19.10 kJ/mol. The ΔG values were negative for both adsorption and desorption, indicating that the adsorption and desorption process of CAP onto biochar was spontaneous and thermodynamically favorable.

3.3. Adsorption isotherms

3.3.1. Freundlich model

The mechanism of the adsorption interaction was investigated using two models, which were the Freundlich model and the Langmuir model.

The Freundlich model is commonly used to analyze non-uniform adsorption behavior, and it is assumed that the adsorption behavior is a multi-layer adsorption process that occurs on heterogeneous surfaces [64]. According to equation (3), the Freundlich distribution models of lg q_e versus lg C_e for different sorbents are shown in Fig. 5 and Table S3. The correlation coefficients (R^2) ranged from 0.86 to 0.96, and all the values were larger than 0.85. The results showed that the adsorption procedure fitted Freundlich model well.

3.3.2. Langmuir model

The Langmuir model is used intensely in adsorption studies to make a comparison between the adsorption capacities of different adsorbents in order to evaluate the efficiency of these adsorbents. It is assumed that the adsorption behavior is a mono-layer adsorption process and the adsorption rate is proportional to the WSB empty spaces and the concentration of CAP in the solution. According to equation (4), the Langmuir distribution models of $1/q_e$ versus $1/C_e$ for different sorbents are shown in Fig. 6 and Table S4. The correlation coefficients (R^2) ranged from 0.89 to 0.99, and all the values were larger than 0.85. The results showed that the adsorption procedure also fitted Langmuir model well.

The Freundlich and Langmuir constants and correlation coefficients for the CAP adsorption are shown in Table 2.

In Freundlich model analysis, when the value of 1/n is greater than one, it means that the isothermal adsorption line belongs to the S style. When the value of 1/n is equal to one, it means that the isothermal adsorption line belongs to linear adsorption. When the value of 1/n is less than one, it means that the isothermal adsorption line belongs to the L style. Table 2 showed that for the soil only, the value of 1/n was greater than one, which means that the CAP isothermal adsorption line belonged to the S style. The WSB addition in the soil changed the isothermal adsorption line from S style to L style. Additionally, in Freundlich model analysis, the lgK_f value indicates the adsorption capacity of the adsorbent, and the adsorption capacity increased with an increase in the lgK_f values. Table 2 showed that the lgK_f value ranges from 0.64 to 1.64, and the value of the soil was the minimum. The lgK_f value increased as the proportion of the biomass charcoal added increased. This demonstrated that the WSB addition in the soil increased its CAP adsorption capacity. The Freundlich model analysis was performed to explain the following two assumptions: (i) the adsorption behavior was single layer adsorption or multi-layer adsorption; and (ii) the adsorption process belonged to a physical or chemical process. However, the Freundlich model could not distinguish between monolayer adsorption and multilayer adsorption, and it was also troublesome for providing the range and magnitude of nonlinear adsorption [65–67].

Table 2 shows that the correlation coefficients (R^2) using the Langmuir model ranges from 0.89 to 0.99, and were all greater than 0.85. The R^2 using the Freundlich model ranges from 0.86 to 0.98. All the R^2 values from Langmuir model are greater than that from the Freundlich model. The results showed that the Langmuir model fitted the data better than the Freundlich model, and this indicated

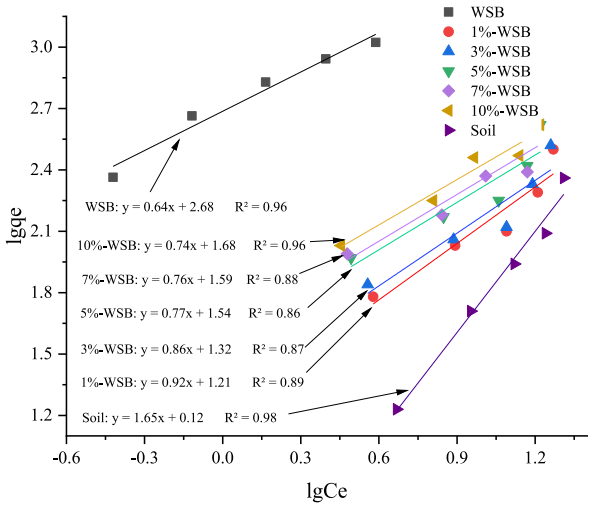

Fig. 5. Freundlich distribution model of lg q_e and lg C_e for CAP/soil at 298 K (a. WSB, b.1%-WSB addition, c. 3%-WSB addition, d. 5%-WSB addition, e. 7%-WSB addition, f. 10%-WSB addition, g. Soil).

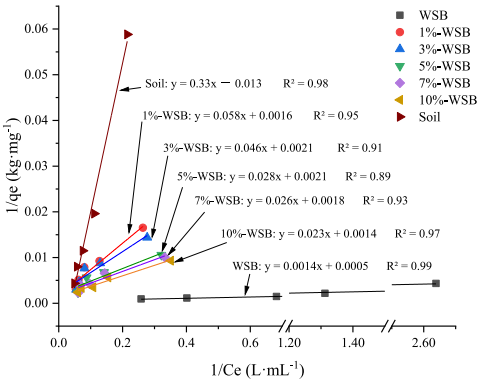

Fig. 6. Langmuir distribution model of $1/q_e$ and $1/C_e$ for CAP/soil at 298 K (a. WSB, b. 1%-WSB addition, c. 3%-WSB addition, d. 5%-WSB addition, e. 7%-WSB addition, f. 10%-WSB addition, g. Soil).

Table 2
Freundlich and Langmuir constants and correlation coefficients for CAP adsorption on WSB.

Soil-biochar type	Freundlich			Langmuir		
	lgK_f	1/n	R^2	Q_{max} (mg/kg)	K_L	R^2
WSB	2.68	0.64	0.96	2000.00	0.35	0.99
1%-WSB	1.21	0.92	0.89	625.01	0.027	0.95
3%-WSB	1.31	0.86	0.87	476.21	0.045	0.91
5%-WSB	1.54	0.77	0.86	476.22	0.076	0.89
7%-WSB	1.59	0.76	0.88	555.60	0.070	0.93
10%-WSB	1.68	0.73	0.96	714.30	0.60	0.97
Soil	0.12	1.64	0.98	−79.36	−0.038	0.98

that the adsorption behavior was a mono-layer adsorption process.

3.4. Adsorption action analysis of CAP on the WSB

The adsorption isotherm is a macroscopic manifestation of the adsorption behavior, and its shape and type can roughly reflect the type of adsorption. The Freundlich model analysis showed that with the WSB addition in soil, the adsorption behavior for CAP changed from the S style to the L style, the adsorption ability increased, and the proportion of CAP increased.

The adsorption isotherms fitted the Freundlich model well, and it also showed that the two models could imitate the adsorption behavior of CAP on soil. The adsorption behavior of CAP on soil was S style, and this indicated that the adsorption capacity of the soil for water molecules was stronger than that for the CAP molecules. When WSB added, the adsorption behavior of the soil/WSB on CAP changed to the L style, and this indicated that WSB had a strong adsorption ability for CAP. The lgK_f values in Freundlich model and K_L values in Langmuir model can both indicate adsorption ability, and the bigger the value, the stronger of the adsorption ability. An analysis of the fitting results of these two models showed that for the adsorption ability of CAP, the order was as follows: WSB >10%-WSB >7%-WSB >5%-WSB >3%-WSB >1%-WSB > soil.

3.5. Mechanism of WSB to remove CAP on theory

The characterization analysis of the WSB showed that there was a large amount of lignin remained in the WSB. In addition, the functional groups of alkyl carbon, methoxyl carbon, aromatic carbon, and carboayl carbon and molecular bonds, such as C-H, -OH, C=C, and C=O, existed in the WSB. Previous studies have shown that the π-π electron donor acceptor interaction, the electrostatic interaction of humic substances in soil, and π-H-bonding are the primary adsorption sites of WSB adsorption.

The adsorption mechanism of biochar for pesticides was related to the specific surface area, richness of surface functional groups, pore structure of the biomass charcoal, intermolecular forces between the biochar and pesticides, and the chemical intermolecular force. According to the sorption equilibrium of the CAP results, CAP would reach a balance in a short time (10 min), and the primary reason is because WSB adsorption in the soil and the concentration in water decrease. Because the adsorption time was short, it was ruled out that the concentration reduction was caused by the degradation of CAP itself.

When the WSB was combined with soil, the adsorption ability increased, and the adsorption ability was greater than that of the WSB itself. The results showed that the accumulation of functional groups on the surface of the biochar itself generated intermolecular

forces that reduced the adsorption sites for pesticides. After mixing the WSB with soil, the potential binding sites between the WSB and pesticides opened, and the adsorption capacity of pesticides increased.

3.6. Use guide of WSB to remove CAP

The adsorption thermodynamic results showed that under the 298 K test conditions, for soil and WSB and in soils with different proportions of the WSB addition, the CAP adsorption of the soil/WSB occurred spontaneously. In addition, the degree of spontaneous reaction from strong to weak was in the following order: 5%-WSB >7%-WSB >10%-WSB >1%-WSB >3%-WSB > soil > WSB. When there was only WSB, the adsorption kinetic energy of the WSB was less than that of the mixture of soil and WSB. This may have been because the adsorption kinetic energy of WSB only was less than that of the mixture of WSB and soil. In agricultural production applications, it is suggested to use 5 % (m/m) WSB application for CAP pollution control to achieve the best economic benefits.

4. Conclusion

WSB contained a large amount of lignin charcoal including alkyl carbon, methoxyl carbon, aromatic carbon, and carboayl carbon, and these lignin charcoal functional groups made electron donor acceptor interaction possible and enhanced the adsorption ability of sorbents. Batch equilibrium study showed WSB application in soil significantly improved the adsorption ability for CAP. The adsorption isotherm analysis showed that the Langmuir model fitted the data better than the Freundlich model,and this indicated that the adsorption behavior was a mono-layer adsorption process. In contrast, the Freundlich model analysis showed that the WSB addition to the soil increased its CAP adsorption capacity, as evidenced by the increase in the lgK_f values. Under the 298 K test conditions, the adsorption thermodynamic results showed that, for soil, the CAP adsorption on the soil/WSB occurred spontaneously. The degree of spontaneous reaction from strong to weak was in the following order: 5%-WSB >7%-WSB >10%-WSB >1%-WSB >3%-WSB > soil > WSB. With a 5 % WSB application, the mixture of WSB and soil showed the best adsorption kinetic energy. The CAP adsorption ability on soil/WSB is affected by the accumulation of functional groups on the surface of the itself, and this generated intermolecular forces that reduced the adsorption sites for pesticides. However, after mixing WSB with soil, the potential binding sites between the WSB and pesticides opened, and the adsorption capacity of pesticides increased. The mixture of WSB and soil with appropriate proportion is helpful to enhance WSB adsorption ability and is economically feasible in production. It is suggested to use 5 % (m/m) WSB application for CAP pollution control in agricultural production.

CRediT authorship contribution statement

Caixia Sun: Writing – review & editing, Project administration, Funding acquisition. **Gangjun Wang:** Formal analysis. **Yuhong Liu:** Writing – original draft. **Ke Bei:** Software. **Guoguang Yu:** Methodology. **Weiran Zheng:** Software, Investigation. **Yuxue Liu:** Writing – review & editing, Data curation.

Statements and declarations

Ethical approval and consent to participate

Not applicable. All authors have read, understood, and complied as applicable with the statement on "Ethical responsibilities of Authors", as found in the Instructions for Authors.

Consent to publish

Not applicable.

Data availability

All data generated or analyzed during this study are included in this article and its supplementary information files.

Funding

This work was supported by the Ministry of Science and Technology of the People's Republic of China for its invaluable support through the National Key R&D Program of China (2018YFF0213406 & 2018YFF0213505).

Declaration of competing interest

The authors declare that they have no known competing financial interests or personal relationships that could have appeared to influence the work reported in this paper.

Acknowledgments

The authors would like to thank Professor Shengmao Yang (Biomass Carbon Engineering Center of the Zhejiang Academy of Agricultural Sciences) for providing the rice straw biochar sample. We thank LetPub (www.letpub.com) for its linguistic assistance during the preparation of this manuscript.

Appendix A. Supplementary data

Supplementary data to this article can be found online at https://doi.org/10.1016/j.heliyon.2024.e39123.

References

[1] X.J. Li, H. Jiang, J.Z. Wu, F. Zheng, K.J. Xu, Y.G. Lin, et al., Drip application of chlorantraniliprole effectively controls invasive Spodoptera frugiperda (Lepidoptera: noctuidae) and its distribution in maize in China, Crop Prot 143 (2021) 105474, https://doi.org/10.1016/j.cropro.2020.105474.
[2] X.J. Li, M.L. Tu, B.X. Yang, Q.H. Zhang, H.M. Li, W. Ma, Chlorantraniliprole in foods: determination, dissipation and decontamination, Food Chem. 406 (2023) 135030, https://doi.org/10.1016/j.foodchem.2022.135030.
[3] Y.B. Wei, R. Yan, Q.L. Zhou, L.Y. Qiao, G.N. Zhu, M.L. Chen, Monitoring and mechanisms of chlorantraniliprole resistance in chilo suppressalis (Lepidoptera: crambidae) in China, J. Econ. Entomol. 112 (2019) 1348–1353, https://doi.org/10.1093/jee/toz001.
[4] C. Cheng, J. Hu, Residue levels of chlorantraniliprole and clothianidin in rice and sugar cane and chronic dietary risk assessment for different populations, Microchem. J. 183 (2022) 107936, https://doi.org/10.1016/j.microc.2022.107936.
[5] S.H. Yang, H. Choi, Insecticides chlorantraniliprole and flubendiamide in Aster scaber: dissipation kinetics, processing effects, and risk assessment, Heliyon 10 (2024) e33216, https://doi.org/10.1016/j.heliyon.2024.e33216.
[6] L. Xu, J. Zhao, D.J. Xu, G.C. Xu, Y.C. Peng, Y.N. Zhang, New insights into chlorantraniliprole metabolic resistance mechanisms mediated by the striped rice borer cytochrome P450 monooxygenases: a case study of metabolic differences, Sci. Total Environ. 912 (2024) 169229, https://doi.org/10.1016/j.scitotenv.2023.169229.
[7] C. Wu, S. Zhang, G. Nie, Z. Zhang, J. Wang, Adsorption and desorption of herbicide monosulfuron-ester in Chinese soils, J. Environ. Sci. 23 (2011) 1524–1532, https://doi.org/10.1016/s1001-0742(10)60583-9.
[8] B.J. Xu, K. Wang, N. Vasylieva, H. Zhou, X.L. Xue, B.M. Wang, et al., Development of a nanobody-based ELISA for the detection of the insecticides cyantraniliprole and chlorantraniliprole in soil and the vegetable bok choy, Anal. Bioanal. Chem. 413 (2021) 2503–2511, https://doi.org/10.1007/s00216-021-03205-x.
[9] C.N. Wang, Y.F. Qin, Y.L. Li, R.L. Wu, D.Q. Zhu, F. Zhou, et al., Variations of root-associated bacterial cooccurrence relationships in paddy soils under chlorantraniliprole (CAP) stress, Sci. Total Environ. 779 (2021) 146247, https://doi.org/10.1016/j.scitotenv.2021.146247.
[10] M. Bertola, A. Ferrarini, G. Visioli, Improvement of soil microbial diversity through sustainable agricultural practices and its evaluation by -omics approaches: a perspective for the environment, food quality and human safety, Microorganisms 9 (2021) 1400, https://doi.org/10.3390/microorganisms9071400.
[11] A. Kowalska, A. Grobelak, A.R. Almas, B.R. Singh, Effect of biowastes on soil remediation, plant productivity and soil organic carbon sequestration: a review, Energies 13 (2020) 5813, https://doi.org/10.3390/en13215813.
[12] R.D. Bardgett, W.H. Van Der Putten, Belowground biodiversity and ecosystem functioning, Nature 515 (2014) 505–511, https://doi.org/10.1038/nature13855.
[13] G.S. Toor, Y.Y. Yang, S. Das, S. Dorsey, G. Felton, Soil health in agricultural ecosystems: current status and future perspectives, Adv. Agron. 168 (2021) 157–201, https://doi.org/10.1016/bs.agron.2021.02.004.
[14] Y. Zhou, Z.Y. Zhang, J. Jing, F.F. Bao, L.X. Wu, Y.H. Du, et al., Integrating environmental carry capacity based on pesticide risk assessment in soil management: a case study for China, J. Hazard Mater. 460 (2023) 132341, https://doi.org/10.1016/j.jhazmat.2023.132341.
[15] W.B. Tseng, M.M. Hsieh, C.H. Chen, T.C. Chiu, W.L. Tseng, Functionalized gold nanoparticles for sensing of pesticides: a review, J. Food Drug Anal. 28 (2020) 521–538, https://doi.org/10.38212/2224-6614.1092.
[16] E. Ko, M. Choi, S. Shin, Bottom-line mechanism of organochlorine pesticides on mitochondria dysfunction linked with type 2 diabetes, J. Hazard Mater. 393 (2020) 122400, https://doi.org/10.1016/j.jhazmat.2020.122400.
[17] E.D. Ongley, Control of water pollution from agriculture. FAO Irrigation and Drainage Paper 55, 1996.
[18] Z.C. Redman, C. Anastasio, R.S. Tjeerdema, Quantum yield for the aqueous photochemical degradation of chlorantraniliprole and simulation of its environmental fate in a model California rice field, Environ. Toxicol. Chem. 39 (2020) 1929–1935, https://doi.org/10.1002/etc.4827.
[19] T.C. Lai, J. Su, Effects of chlorantraniliprole on development and reproduction of beet armyworm, Spodoptera exigua (Hubner), J. Pest, Sci. 84 (2011) 381–386, https://doi.org/10.1007/s10340-011-0366-1.
[20] Q. Tang, P.P. Wang, H.J. Liu, D.C. Jin, X.N. Chen, L.F. Zhu, Effect of chlorantraniliprole on soil bacterial and fungal diversity and community structure, Heliyon 9 (2023) e13668, https://doi.org/10.1016/j.heliyon.2023.e13668.
[21] S. Sur, M. Sathiavelu, A concise overview on pesticide detection and degradation strategies, Env. Pollut. Bioavail. 34 (2022) 112–116, https://doi.org/10.1080/26395940.2022.2041489.
[22] J.P. Verma, D.K. Jaiswal, R. Sagar, Pesticide relevance and their microbial degradation: a-state-of-art, Rev. Environ. Sci. Bio. 13 (2014) 429–466, https://doi.org/10.1007/s11157-014-9341-7.
[23] S.G. Parte, A.D. Mohekar, A.S. Kharat, Microbial degradation of pesticide: a review, Afr. J. Microbiol. Res. 11 (2017) 992–1012, https://doi.org/10.5897/ajmr2016.8402.
[24] M.K. Awasthi, S. Sarsaiya, S. Wainaina, K. Rajendran, S.K. Awasthi, T. Liu, et al., Techno-economics and life-cycle assessment of biological and thermochemical treatment of bio-waste, Renew. Sustain. Energy Rev. 144 (2021) 110837, https://doi.org/10.1016/j.rser.2021.110837.
[25] A. Susilawati, E. Maftuah, A. Fahmi, The utilization of agricultural waste as biochar for optimizing swampland: a review, IOP Conf. Ser. Mater. Sci. Eng. 980 (2020) 012065, https://doi.org/10.1088/1757-899X/980/1/012065.
[26] L.J. Leng, Q. Xiong, L.H. Yang, H. Li, Y.Y. Zhou, W.J. Zhang, et al., An overview on engineering the surface area and porosity of biochar, Sci. Total Environ. 763 (2021) 144204, https://doi.org/10.1016/j.scitotenv.2020.144204.
[27] Y. Ding, Y.G. Liu, S.B. Liu, Z.W. Li, X.F. Tan, X.X. Huang, et al., Biochar to improve soil fertility. A review, Agron. Sustain. Dev. 36 (2016) 36, https://doi.org/10.1007/s13593-016-0372-z.
[28] X.Y. Yu, L.G. Pan, G.G. Ying, R.S. Kookana, Enhanced and irreversible sorption of pesticide pyrimethanil by soil amended with biochars, J. Environ. Sci. 22 (2010) 615–620, https://doi.org/10.1016/S1001-0742(09)60153-4.
[29] Y.C. Li, Y.F. Li, S.X. Chang, Y.F. Yang, S.L. Fu, P.K. Jiang, et al., Biochar reduces soil heterotrophic respiration in a subtropical plantation through increasing soil organic carbon recalcitrancy and decreasing carbon degrading microbial activity, Soil Biol. Biochem. 122 (2018) 173–185, https://doi.org/10.1016/j.soilbio.2018.04.019.
[30] Y.X. Liu, L. Lonappan, S.K. Brar, S.M. Yang, Impact of biochar amendment in agricultural soils on the sorption, desorption, and degradation of pesticides: a review, Sci. Total Environ. 645 (2018) 60–70, https://doi.org/10.1016/j.scitotenv.2018.07.099.

[31] T.T. Wang, J. Cheng, X.Y. Liu, W.N. Jiang, C.L. Zhang, X.Y. Yu, Effect of biochar amendment on the bioavailability of pesticide chlorantraniliprole in soil to earthworm, Ecotoxicol. Environ. Saf. 83 (2012) 96–101, https://doi.org/10.1016/j.ecoenv.2012.06.012.

[32] K. Abas, J. Brisson, M. Amyot, J. Brodeur, V. Storck, J.M. Montiel-León, et al., Effects of plants and biochar on the performance of treatment wetlands for removal of the pesticide chlorantraniliprole from agricultural runoff, Ecol. Eng. 175 (2022) 106477, https://doi.org/10.1016/j.ecoleng.2021.106477.

[33] S. Aniruddha, Y. Ji-Hyock, J. Won-Tae, Environmental fate and metabolic transformation of two non-ionic pesticides in soil: effect of biochar, moisture, and soil sterilization, Chemosphere 349 (2023) 140965, https://doi.org/10.1016/j.chemosphere.2023.140458.

[34] H.G. Cheng, D. Xing, S. Lin, Z.X. Deng, X. Wang, W.J. Ning, et al., Iron-modified biochar strengthens simazine adsorption and decreases simazine decomposition in the soil, Front. Microbiol. 13 (2022) 1–10, https://doi.org/10.3389/fmicb.2022.901658.

[35] X.W. You, H.T. Jiang, M. Zhao, F.Y. Suo, C.S. Zhang, H. Zheng, et al., Biochar reduced Chinese chive (Allium tuberosum) uptake and dissipation of thiamethoxam in an agricultural soil, J. Hazard Mater. 390 (2020) 121749, https://doi.org/10.1016/j.jhazmat.2019.121749.

[36] S. Khalid, M. Shahid, B. Murtaza, I. Bibi, Natasha, M.A. Naeem, et al., A critical review of different factors governing the fate of pesticides in soil under biochar application, Sci. Total Environ. 711 (2020) 134645, https://doi.org/10.1016/j.scitotenv.2019.134645.

[37] S. Azizian, M. Haerifar, J. Basiri-Parsa, Extended geometric method: a simple approach to derive adsorption rate constants of Langmuir-Freundlich kinetics, Chemosphere 68 (2007) 2040–2046, https://doi.org/10.1016/j.chemosphere.2007.02.042.

[38] Y.Z. Cheng, B.Y. Wang, J.M. Shen, P.W. Yan, J. Kang, W.Q. Wang, et al., Preparation of novel N-doped biochar and its high adsorption capacity for atrazine based on π-π electron donor-acceptor interaction, J. Hazard Mater. 432 (2022) 128757, https://doi.org/10.1016/j.jhazmat.2022.128757.

[39] P. Zhang, C. Ren, H. Sun, L. Min, Sorption, desorption and degradation of neonicotinoids in four agricultural soils and their effects on soil microorganisms, Sci. Total Environ. 615 (2018) 59–69, https://doi.org/10.1016/j.scitotenv.2017.09.097.

[40] H.J. Hu, J. Meng, H. Zheng, H.Q. Cai, M.X. Wang, Z.B. Luo, et al., Relief effect of biochar on continuous cropping of tobacco through the reduction of p-hydroxybenzoic acid in soil, Heliyon 10 (2024) e33011, https://doi.org/10.1016/j.heliyon.2024.e33011.

[41] M. Zaheer, M.S. Ali, N. Huang, M.A. Ashraf, Using walnut shells as low-cost adsorbent materials in an anaerobic filter medium of a De-centralized wastewater treatment system (DEWATS), Chemosphere 341 (2023) 140080, https://doi.org/10.1016/j.chemosphere.2023.140080.

[42] D. Kim, S. Cho, J.J. Jeon, J. Choi, Inhalation toxicity screening of consumer products chemicals using OECD test guideline data-based machine learning models, J. Hazard Mater. 478 (2024) 135446, https://doi.org/10.1016/j.jhazmat.2024.135446.

[43] H.B. Li, X.L. Dong, E.B. da Silva, L.M. de Oliveira, Y.S. Chen, L.N.Q. Ma, Mechanisms of metal sorption by biochars: biochar characteristics and modifications, Chemosphere 178 (2017) 466–478, https://doi.org/10.1016/j.chemosphere.2017.03.072.

[44] OCED, OECD Giuidline for Testing of Chemicals, Adsorption - Desorption Using a Batch Equilibrium Method, 2000.

[45] B.M.D.E. Castro, L.C. Martínez, A. Plata-Rueda, M.A. Soares, C.F. Wilcken, A.J.V. Zanuncio, et al., Exposure to chlorantraniliprole reduces locomotion, respiration, and causes histological changes in the midgut of velvetbean caterpillar Anticarsia gemmatalis (Lepidoptera: noctuidae), Chemosphere 263 (2021) 128008, https://doi.org/10.1016/j.chemosphere.2020.128008.

[46] X. Dong, Y. Chu, Z. Tong, M.N. Sun, D.D. Meng, X.T. Yi, et al., Mechanisms of adsorption and functionalization of biochar for pesticides: a review, Ecotox. Environ. Safe. 272 (2024) 116019, https://doi.org/10.1016/j.ecoenv.2024.116019.

[47] H. Deng, D. Feng, J.X. He, F.Z. Li, H.M. Yu, C.J. Ge, Influence of biochar amendments to soil on the mobility of atrazine using sorption-desorption and soil thin-layer chromatography, Ecol. Eng. 99 (2017) 381–390, https://doi.org/10.1016/j.ecoleng.2016.11.021.

[48] H. Cederlund, E. Boerjesson, J. Stenstroem, Effects of a wood-based biochar on the leaching of pesticides chlorpyrifos, diuron, glyphosate and MCPA, J. Environ. Manage. 191 (2017) 28–34, https://doi.org/10.1016/j.jenvman.2017.01.004.

[49] M.A.S. Holanda, J.M.C. Menezes, H.D.M. Coutinho, R.N.P. Teixeira, Effectiveness of biochar as an adsorbent for pesticides: systematic review and meta-analysis, J. Environ. Manage. 345 (2023) 118719, https://doi.org/10.1016/j.jenvman.2023.118719.

[50] L.Y. Yang, X.Y. Yang, J.T. Guo, Z.Y. Yang, Y.H. Du, Q.Q. Lu, et al., Invasive plant-derived biochar for sustainable bioremediation of pesticide contaminated soil, Chem. Eng. J. 487 (2024) 148689, https://doi.org/10.1016/j.cej.2024.148689.

[51] Y.J. Dai, Y.F. Liu, Y.L. Wang, W.Y. Fang, Y.M. Chen, Y.Y. Sui, A practice of conservation tillage in the Mollisol region in Heilongjiang Province of China: a mini review, Pol. J. Environ. Studies 32 (2023) 1479–1489, https://doi.org/10.15244/pjoes/156473.

[52] C. Li, Z.F. Yang, T. Yu, Q.Y. Hou, X. Liu, J. Wang, et al., Study on safe usage of agricultural land in karst and non-karst areas based on soil Cd and prediction of Cd in rice: a case study of Heng County, Guangxi, Ecotox, Environ. Safe. 208 (2021) 111505, https://doi.org/10.1016/j.ecoenv.2020.111505.

[53] D.W. Nelson, L.E. Sommers, Total carbon, organic carbon, and organic, Matter (1996) 961–1010, https://doi.org/10.2136/sssabookser5.3.c34.

[54] N. Abdullah, R.M. Taib, N.S.M. Aziz, M.R. Omar, N.M. Disa, Banana pseudo-stem biochar derived from slow and fast pyrolysis process, Heliyon 9 (2023) e12940, https://doi.org/10.1016/j.heliyon.2023.e12940.

[55] D.D. Li, X.Y. Zhang, S.M. Green, J.A.J. Dungait, X.F. Wen, Y.Q. Tang, et al., Nitrogen functional gene activity in soil profiles under progressive vegetative recovery after abandonment of agriculture at the Puding Karst Critical Zone Observatory, SW China, Soil Biol. Biochem. 125 (2018) 93–102, https://doi.org/10.1016/j.soilbio.2018.07.004.

[56] D.B. Li, X.J. Li, Y. Tao, Z.N. Yan, Y.S. Ao, Deciphering the bacterial microbiome in response to long-term mercury contaminated soil, Ecotox. Environ. Safe. 229 (2022) 113062, https://doi.org/10.1016/j.ecoenv.2021.113062.

[57] J. Kim, Y.G. Lee, H. Kim, K. Chon, C. Phae, One-step synthesis of magnetic biochar via co-pyrolysis of walnut shells and Fe-rich mine tails for adsorption capacity improvement of polystyrene sulfonate microplastics: role of microplastic size, Environ. Technol. Innovat. 34 (2024) 103624, https://doi.org/10.1016/j.eti.2024.103624.

[58] H.X. Zhu, Y. Teng, X.M. Wang, L. Zhao, W.J. Ren, Y.M. Luo, et al., Changes in clover rhizosphere microbial community and diazotrophs in mercury-contaminated soils, Sci. Total Environ. 767 (2021) 145473, https://doi.org/10.1016/j.scitotenv.2021.145473.

[59] H.P. Xie, M.Z. Gao, C.B. Li, D.L. Shang, Q.Q. Liu, Influence of desorption hysteresis effects on coalbed methane migration and production based on dual-porosity medium model incorporating hysteresis pressure, Comput. Geotech. 165 (2024) 105893, https://doi.org/10.1016/j.compgeo.2023.105893.

[60] N. Bahramifar, M. Tavasolli, H. Younesi, Removal of eosin Y and eosin B dyes from polluted water through biosorption using Saccharomyces cerevisiae: isotherm, kinetic and thermodynamic studies, J. Appl. Res. Wat. Wast. 3 (2015) 108–114.

[61] M.M. Chen, Z. Yan, J.D. Luan, X. Sun, W.G. Liu, X. Ke, π-π electron-donor-acceptor (EDA) interaction enhancing adsorption of tetracycline on 3D PPY/CMC aerogels, Chem. Eng. J. 454 (2023) 140300, https://doi.org/10.1016/j.cej.2022.140300.

[62] J.G. Du, J. Chen, C.Y. Zhang, G. Jiang, Screening out the transition metal single atom supported on onion-like carbon(OLC) for the hydrogen evolution reaction, Inorg. Chem. 62 (2023) 1001–1006, https://doi.org/10.1021/acs.inorgchem.2c03922.

[63] M.C. Carter, J.E. Kilduff, W.J. Weber, Site energy distribution analysis of preloaded adsorbents, Environ. Sci. Technol. 29 (1995) 1773–1780, https://doi.org/10.1021/es00007a013.

[64] M. Vigdorowitsch, A. Pchelintsev, L. Tsygankova, E. Tanygina, Freundlich isotherm: an adsorption model complete framework, Appl. Sci. Basel 11 (2021), https://doi.org/10.3390/app11178078.

[65] M. Wu, G.L. Li, P.F. Li, N. Jiang, S.P. Wei, E. Petropoulos, et al., Assessing the ecological risk of pesticides should not ignore the impact of their transformation byproducts-The case of chlorantraniliprole, J. Hazard Mater. 418 (2021) 126270, https://doi.org/10.1016/j.jhazmat.2021.126270.

[66] G. Cheng, K.G. Karthikeyan, S.D. Sibley, J.A. Pedersen, Complexation of the antibiotic tetracycline with humic acid, Chemosphere 66 (2007) 1494–1501, https://doi.org/10.1016/j.chemosphere.2006.08.028.

[67] J.D. Wang, L.F. Chen, Y.R. Wang, H.Y. Fu, A. Ali, D. Xiao, et al., Silence of ryanodine receptor gene decreases susceptibility to chlorantraniliprole in the oriental armyworm, Mythimna separata Walker, Pestic. Biochem. Phys. 148 (2018) 34–41, https://doi.org/10.1016/j.pestbp.2018.03.012.